

# How Analytic Choices Can Affect the Extraction of Electromagnetic Form Factors from Elastic Electron Scattering Cross Section Data

Douglas W. Higinbotham and Randall E. McClellan  
*Jefferson Lab, Newport News, VA 23606*

Scientists often try to incorporate prior knowledge into their regression algorithms, such as a particular analytic behavior or a known value at a kinematic endpoint. Unfortunately, there is often no unique way to make use of this prior knowledge, and thus, different analytic choices can lead to very different regression results from the same set of data. To illustrate this point in the context of the proton electromagnetic form factors, we use the Mainz elastic data with its 1422 cross section points and 31 normalization parameters. Starting from a complex unconstrained non-linear regression, we will show how the addition of a single, theory-motivated constraint removes an oscillation from the magnetic form factor and shifts the extracted proton charge radius. We then repeat both regressions using the same algorithm, but with a rebinned version of the Mainz data set. These examples illustrate how analytic choices, such as the function that is being used or even the binning of the data, can dramatically affect the results of a complex regression and show why it is critical to have either a physical model in mind or firm mathematical basis when designing regression algorithms.

Keywords: form factors; proton radius; confirmation bias; regression

## I. INTRODUCTION

Silberzahn *et al.* [1] points out that there is often little appreciation for how different analytic strategies can affect a reported result. In this work, we illustrate how these analytic choices can impact the extraction of the electromagnetic form factors from electron scattering data. Extractions are frequently done with complex non-linear regression algorithms and tend to make use of prior information about the limiting behavior of the electromagnetic form factors through the use of floating normalization parameters. Since shifts of the normalization parameters can affect the physical parameters of interest, these parameters can have a large impact on the interpretation of the experimental data. Also, scientists tend to look at all regressions as being the same, when in fact there are many different types of regression models such as descriptive, predictive and explanatory [2]. Though the type of regression model being developed is not always clearly stated, it is yet another choice that affects how the scientist design their regression algorithms. These choices can create differences in the interpretation of the data that are far larger than any other source of uncertainty.

## II. PROTON ELASTIC SCATTERING

There has been a renewed interest in low  $Q^2$  proton elastic scattering data due to muonic hydrogen Lamb shift results that determined the charge radius of the proton to be 0.84078(39) fm [3, 4], a result in stark contrast to the current recommended CODATA value of 0.8751(61) fm [5]. This systematic difference has become known as the proton radius puzzle [6–8].

For electron scattering data, the proton charge radius,  $r_p$ , is extracted from the cross sections by determining

the slope of the electric form factor,  $G_E$ , in the limit of four-moment transfer,  $Q^2$ , approaching zero [9]:

$$r_p \equiv \left( -6 \left. \frac{dG_E(Q^2)}{dQ^2} \right|_{Q^2=0} \right)^{1/2}. \quad (1)$$

Since the scattering data is measured at finite  $Q^2$ , an extrapolation is required to extract the charge radius. Authors have taken many different approaches to this extraction, yielding systematically different outcomes [10–18].

To clearly illustrate how analytic choice can strongly affect the extracted radius, we use the full 1422 point Mainz data set along with its 31 normalization parameters and fit it with complex non-linear regression with 53 free parameters that is very similar to the original Mainz approach [19, 20]. We next repeat the regression with the one added requirement that the electromagnetic form factors be “completely monotone” functions: functions  $f$  that possess derivatives  $f^n$  of all orders such that  $(-1)^n f^n(x) \geq 0, x > 0$  [21]. The standard dipole function, which is often used as an approximation of the electron magnetic form factors, is an example of a completely monotone function, as are most theory motivated form factors. In statistics terms, adding the condition that the function be completely monotone would be classified as creating a robust regression model [22]. Ideally, these regression models would have been carefully developed prior to obtaining the experimental data, as done by the PRad collaboration [23]; otherwise, as we will show, one must be exceedingly careful to avoid confirmation bias [24, 25].

### III. CROSS SECTION FORMULAS

In the plane-wave Born approximation, the cross section for elastic electron scattering on a proton is given by

$$\sigma = \sigma_{\text{Mott}} \times \left[ \frac{G_E^2(Q^2) + \tau G_M^2(Q^2)}{1 + \tau} + 2\tau G_M^2(Q^2) \tan^2 \frac{\theta}{2} \right] \quad (2)$$

where  $\tau = \frac{Q^2}{4m_p^2}$  with  $Q^2 = 4E_{\text{Beam}}E' \sin^2 \frac{\theta}{2}$  and  $E_{\text{Beam}}$  is the energy of the electron beam,  $E'$  is the energy of the outgoing electron,  $\theta$  is the scattering angle of the outgoing electron, and  $m_p$  is the mass of the proton. For the purpose of making a descriptive model of experimental data, the form factors can be parameterized in terms of an  $n^{\text{th}}$  order polynomial

$$G_{E,\text{polynomial}}(a_i^E, Q^2) = 1 + \sum_{i=1}^n a_i^E Q^{2i} \quad (3)$$

$$G_{M,\text{polynomial}}(a_i^M, Q^2) = \mu_p \left( 1 + \sum_{i=1}^n a_i^M Q^{2i} \right) \quad (4)$$

where  $\mu_p$  is the magnetic moment of the proton.

### IV. NORMALIZATION PARAMETERS

As noted in the work of Bernauer *et al.* [20], knowledge of the absolute value of cross sections is limited by determination of the absolute luminosity. In order to reduce the normalization uncertainty, the original fits of this data made use of prior knowledge of the form factors in the limit of  $Q^2 = 0$ . This brings a model dependence to the analysis that is not easily understood, as 31 normalization parameters were incorporated. These parameters are taken in combinations to link sets of data together, with the final value of each cross section point defined by:

$$\sigma_{exp} = \sigma_p \cdot \text{normA}_p \cdot \text{normB}_p, \quad (5)$$

where  $\text{normA}_p$  and  $\text{normB}_p$  are the two normalization parameters associated with that data point. A complete list of the 31 different normalization parameters,  $N_k$ , that are taken in 34 unique combinations for the 1422 points, is shown in Table I. Further details of how these parameters connect to each of the 1422 cross section points can be found in the supplemental material of Bernauer *et al.* [20].

### V. REGRESSIONS

To show how a single analytic change can affect the values of these normalization parameters, we first perform an unconstrained regression where the polynomial

TABLE I. Shown are the 34 different combinations of the 31 normalization parameters,  $N_j$ , found in Ref. [20] which link the data together. Also shown are the number of data points and the  $Q^2$  range of each data set.

Energy	Spec.	normA	normB	Points	$Q^2$ Range [GeV <sup>2</sup> ]
180 MeV	B	N <sub>1</sub>	N <sub>3</sub>	106	0.0038 – 0.0129
	B	N <sub>1</sub>	N <sub>4</sub>	41	0.0101 – 0.0190
	A	N <sub>3</sub>	-	102	0.0112 – 0.0658
	B	N <sub>1</sub>	N <sub>5</sub>	19	0.0190 – 0.0295
	C	N <sub>2</sub>	N <sub>4</sub>	38	0.0421 – 0.0740
C	N <sub>2</sub>	N <sub>5</sub>	17	0.0740 – 0.0834	
315 MeV	B	N <sub>6</sub>	N <sub>9</sub>	104	0.0111 – 0.0489
	A	N <sub>7</sub>	N <sub>9</sub>	38	0.0430 – 0.1391
	A	N <sub>9</sub>	-	40	0.0479 – 0.1441
	C	N <sub>8</sub>	N <sub>9</sub>	62	0.1128 – 0.2131
450 MeV	B	N <sub>10</sub>	N <sub>13</sub>	77	0.0152 – 0.0572
	B	N <sub>10</sub>	N <sub>15</sub>	52	0.0572 – 0.1175
	A	N <sub>13</sub>	-	42	0.0586 – 0.2663
	B	N <sub>10</sub>	N <sub>14</sub>	17	0.0589 – 0.0851
	A	N <sub>11</sub>	N <sub>13</sub>	36	0.0670 – 0.2744
	C	N <sub>12</sub>	N <sub>15</sub>	50	0.2127 – 0.3767
	A	N <sub>14</sub>	-	2	0.2744 – 0.2744
585 MeV	B	N <sub>16</sub>	N <sub>18</sub>	41	0.0255 – 0.0433
	B	N <sub>16</sub>	N <sub>19</sub>	47	0.0433 – 0.1110
	A	N <sub>18</sub>	-	27	0.0590 – 0.0964
	B	N <sub>16</sub>	N <sub>20</sub>	21	0.0920 – 0.1845
	A	N <sub>19</sub>	-	37	0.0964 – 0.4222
	C	N <sub>17</sub>	N <sub>20</sub>	20	0.3340 – 0.5665
720 MeV	B	N <sub>21</sub>	N <sub>25</sub>	47	0.0711 – 0.1564
	A	N <sub>25</sub>	-	46	0.1835 – 0.6761
	C	N <sub>24</sub>	N <sub>26</sub>	28	0.6536 – 0.7603
	A	N <sub>23</sub>	N <sub>26</sub>	27	0.2011 – 0.2520
	A	N <sub>22</sub>	N <sub>26</sub>	37	0.4729 – 0.7474
	A	N <sub>21</sub>	N <sub>26</sub>	36	0.1294 – 0.2435
855 MeV	B	N <sub>27</sub>	N <sub>31</sub>	35	0.3263 – 0.4378
	C	N <sub>28</sub>	N <sub>31</sub>	31	0.7300 – 0.9772
	A	N <sub>29</sub>	N <sub>30</sub>	32	0.3069 – 0.5011
	A	N <sub>29</sub>	-	13	0.5274 – 0.7656
	B	N <sub>27</sub>	N <sub>29</sub>	54	0.0868 – 0.3263

parameters of Eq. 3 and 4 are allowed to vary freely. For the second regression, we constrain the parameters to alternate in sign as one would expect from a completely monotone function. In both cases, we do a weighted least squares minimization with a  $\chi^2$  function defined as follows:

$$\chi^2 = \sum_{p=1}^{p_{max}} \left( \frac{\sigma_{Model}(E_p, \theta_p) - \sigma_p \cdot \text{normA}_p \cdot \text{normB}_p}{\Delta\sigma_p \cdot \text{normA}_p \cdot \text{normB}_p} \right)^2 \quad (6)$$

where for each data point  $p$  there is a cross-section,  $\sigma_p$ , with an energy  $E_p$ , angle  $\theta_p$ , and normalization parameters  $\text{normA}$  and  $\text{normB}$  as shown in Table I. While the

number of degrees of freedom can be estimated for linear models, that is not the case for non-linear models and thus reduced  $\chi^2$  cannot easily be used for interpreting the results of these regressions [26]. As always, one should make plots to check the fit quality [27] particularly since least squares minimizations are very sensitive to outliers.

Also, while regressions that are linear in terms can be solved exactly, this is not the case with non-linear regressions where algorithms can converge in a local or non-physical minimum; thus choosing reasonable initialization parameters is an important step when developing non-linear regression algorithms. Thus, to have reasonable initialization parameters for our complex non-linear regressions, we first performed a regression with a simple dipole functions for  $G_E$  and  $G_M$  with free radius parameters to determine our initial normalization and radius values.

## VI. RESULTS

In Table II and Table III we show the results of fitting with both the constrained and unconstrained regression. These results and residuals are shown graphically in Fig. 1, where for clarity we have divided  $\sigma_{exp}$  by  $\sigma_{dipole}$ , where  $\sigma_{dipole}$  is simply Eq. 2 with standard dipole form factors:

$$G_{E,dipole}(Q^2) = \left(1 + \frac{Q^2}{0.71 \text{ GeV}^2}\right)^{-2}, \quad (7)$$

$$G_{M,dipole}(Q^2) = \mu_p \left(1 + \frac{Q^2}{0.71 \text{ GeV}^2}\right)^{-2}. \quad (8)$$

In Fig. 2 and Fig. 3, we show the individual electron and magnetic form factors obtained from this regression.

Though it is beyond the range of the data used in the regression, the results of regressions like these are frequently used to extract the charge radius of the proton by using Eq. 1 to relate the fit function to the charge radius of the proton. For the case of a polynomial, this is simply

$$r_p = (-6a_1^E)^{-2} \quad (9)$$

and one finds a charge radius of 0.882 fm from the unconstrained regression and 0.854 fm from the constrained. Thus, the unconstrained regression is close to the expected CODATA value while the constrained function is close to the muonic result. With freedom to make analytic choices that so strongly affect the results, there is the potential for confirmation bias and for researchers to select and report the regressions that confirm their expectations [24, 25].

## VII. TOTAL $\chi^2$

For a fixed number of fit parameters, the unbounded regressions presented in this work will always have a total

TABLE II. The values of the polynomial terms for the unconstrained and constrained regressions of the 1422 cross section points following the notation of Eq. 3 and 4. If one wishes to interpret the charge form factor slope term ( $i = 1$ ) in terms of charge radius using Eq. 1, one finds the unbound fit gives a charge radius of 0.882 fm while the bound fit gives a charge radius of 0.854 fm.

i	unbound		bound	
	$a_i^E$	$a_i^M$	$a_i^E$	$a_i^M$
1	-3.33142	-2.52353	-3.12422	-2.79955
2	13.05405	-0.70801	8.82144	5.18800
3	-63.68174	40.15560	-25.73610	-5.74202
4	249.39290	-176.65515	60.05707	2.80554
5	-658.61219	380.27777	-89.41228	-0.00001
6	1099.47817	-392.56122	72.48398	0.01034
7	-987.58975	11.52512	-24.23351	-0.27663
8	57.38266	442.38507	0.00003	0.00000
9	853.41383	-492.08183	-0.00608	-0.00092
10	-810.46435	230.28595	0.00812	0.00127
11	250.37731	-40.91969	-0.00000	-0.00003

$\chi^2$  equal to or lower than a bounded regression as shown in Fig. 4. Since adding parameters will decrease total  $\chi^2$ , by itself it is not a valid model selection criterion. Model selection techniques include using an F-Test for nested models or model selection method like the Akaike Information Criterion (AIC) [28] or the Bayesian Information Criterion (BIC) [29] which can be used with non-nested models (see Ref. [30] for more details).

Modelers should also keep in mind whether they are trying to do a descriptive fit of the data or, by adding physical constraints, building a predictive or explanatory model of the data [2], while also keeping in mind that none of the model selection techniques will prevent the use of completely inappropriate functions. As noted in Ref. [27, 31], it is essential to plot the fit functions and residuals to ensure a reasonable regression as  $\chi^2$  values alone are insufficient.

As a further check of how sensitive these two functions are to the handling of the data in the fit, we use the rebinned version of the Mainz data that is provided in the supplemental material of Ref. [13]. These authors carefully rebinned and re-weighted the full Mainz data and provided new a set of 658 cross section points, though with the same 31 normalization parameters as the original set. By simply replacing the original Mainz data set with this set, we can repeat our regressions. The total  $\chi^2$  values for these polynomial fits are summarized in Fig. 5 and the results and residuals of the 11<sup>th</sup> order regressions are shown in Fig. 6 with the fit parameters given in Table IV. These results show that even just rebinning the data can shift the result of a high-order polynomial regression significantly.

As the changes we have presented in these four fits are larger than the statistical parameter uncertainties, we have limited ourselves to a discussion of the shifts of the

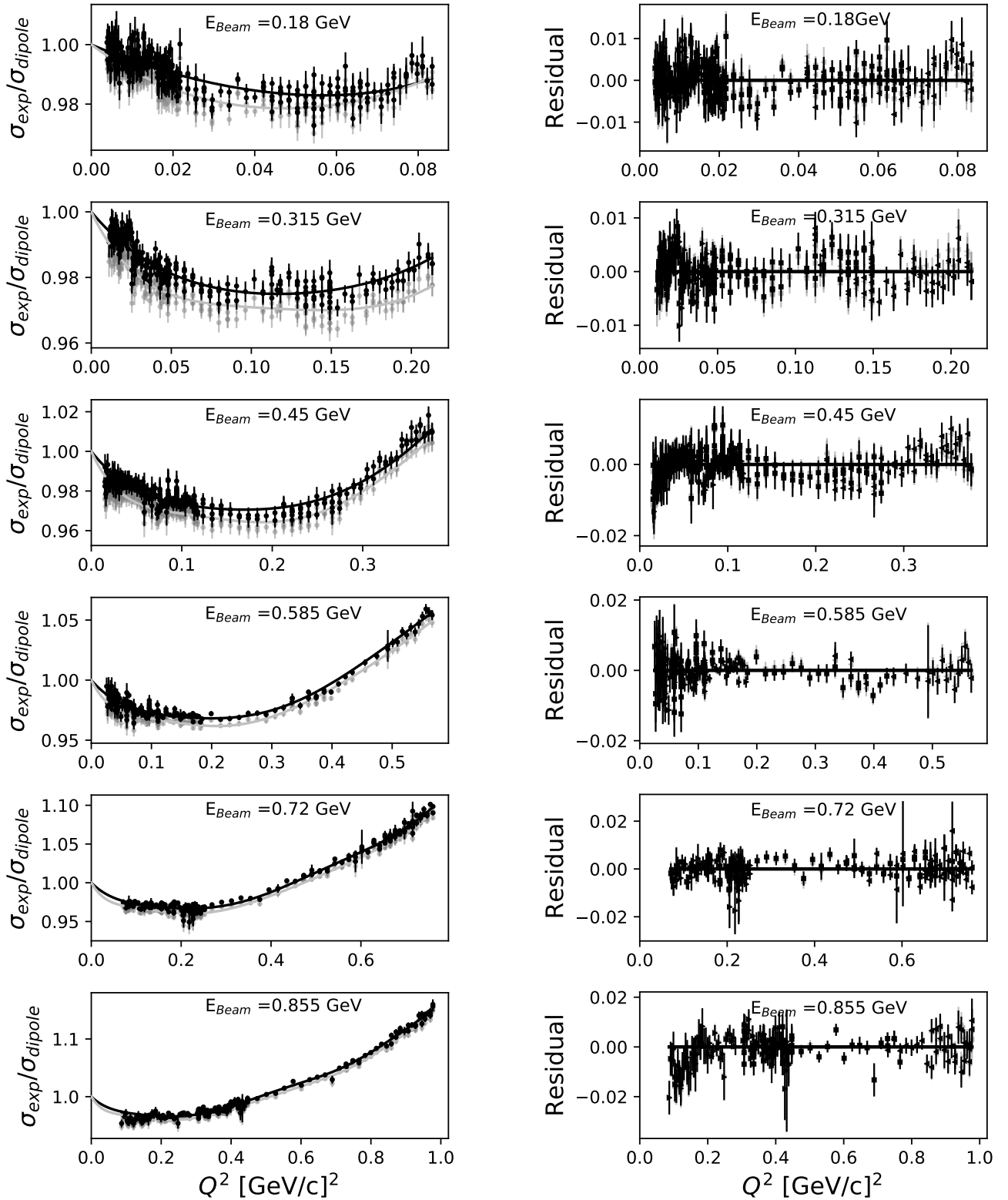


FIG. 1. Shown are the 1422 cross section points analyzed with the two different analytic choices. The grey points were analyzed using an unconstrained eleventh order polynomial in  $G_E$  and  $G_M$  while the black points used a bounded regression constrained to be continuously monotone. The systematic difference in the location of the points is due to how the 31 normalization parameters are affected by the choice of regression function. While these means are different, the residuals of the fits to their respective functions are quite similar.

TABLE III. Shown are the normalization parameters for the unconstrained and constrained regressions along with the difference between them. Compared to the uncertainty of the initial normalizations of a few percent, these changes are all small. More interestingly, since these affect the data in combinations, many of the changes reverse the direction in which the two normalizations change. For example, for the lowest  $Q^2$  data, the normalization is given by  $N_1 \cdot N_4$  which is  $1.00033 \cdot 0.99856$  vs.  $0.99794 \cdot 1.00719$  for the unconstrained and constrained fits, respectively.

	Unconstrained	Constrained	Difference
1	1.00025	0.99848	0.00178
2	1.00045	0.99610	0.00435
3	0.99907	1.00385	-0.00479
4	0.99876	1.00580	-0.00704
5	0.99872	1.00505	-0.00633
6	0.99993	1.00006	-0.00013
7	1.00000	0.99990	0.00010
8	1.00013	1.00087	-0.00074
9	0.99906	1.00497	-0.00591
10	1.00018	1.00084	-0.00065
11	1.00004	1.00009	-0.00005
12	0.99988	1.00076	-0.00087
13	0.99883	1.00471	-0.00588
14	0.99892	1.00445	-0.00552
15	0.99881	1.00337	-0.00456
16	1.00009	1.00042	-0.00033
17	1.00014	1.00102	-0.00088
18	0.99890	1.00520	-0.00630
19	0.99890	1.00423	-0.00533
20	0.99875	1.00382	-0.00507
21	1.00004	0.99935	0.00068
22	0.99944	0.99879	0.00065
23	1.00012	0.99985	0.00027
24	0.99932	0.99833	0.00100
25	0.99879	1.00480	-0.00600
26	0.99907	1.00596	-0.00689
27	1.00063	1.00032	0.00031
28	0.99946	1.00080	-0.00135
29	0.99837	1.00466	-0.00629
30	1.00050	0.99954	0.00096
31	0.99878	1.00398	-0.00520

mean values of the points. For a non-linear regressions such as these, statistical bootstrapping can be used to find the statistical parameter uncertainties.

### VIII. MOMENTS

In some analyses of the proton radius, the values of previously determined fit parameters are used to constrain the fits. For the polynomial regressions, this is done by

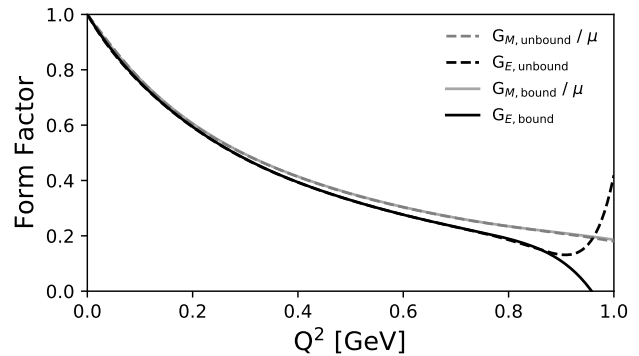


FIG. 2. Shown are the electromagnetic form factors from the unbounded and bounded polynomial regressions to 1422 Mainz cross sections [20]. For these kinematics, as the  $Q^2$  gets large, the cross sections are dominated by  $G_M$  and the  $G_E$  form factor becomes unconstrained, so the divergence at high  $Q^2$  is to be expected from a high-order polynomial.

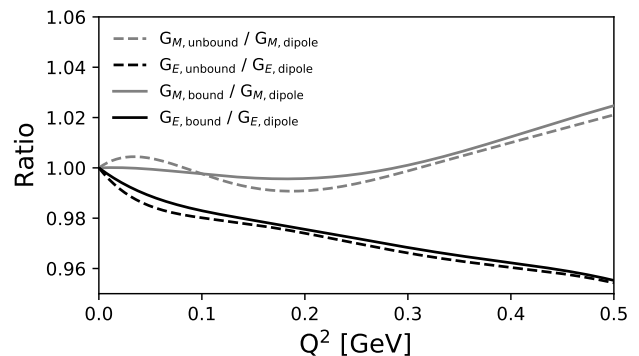


FIG. 3. The ratio of the extracted electromagnetic form factors to standard dipole showing that the oscillation in the magnetic form factor goes away once the fit functions are forced to be continuously monotone. Interestingly, through a complex interplay with the normalization parameters, the smooth magnetic form factor also results in a smaller extracted proton radius (0.854 fm vs. 0.882 fm).

equating the polynomial fit parameters from Eq. 3 and 4 with moments of the underlying true form factors via the following equations:

$$G_E(Q^2) = 1 - \frac{\langle r^2 \rangle_E}{3!} Q^2 + \frac{\langle r^4 \rangle_E}{5!} Q^4 - \frac{\langle r^6 \rangle_E}{7!} Q^6 + \dots (10)$$

$$\frac{G_M(Q^2)}{\mu} = 1 - \frac{\langle r^2 \rangle_M}{3!} Q^2 + \frac{\langle r^4 \rangle_M}{5!} Q^4 - \frac{\langle r^6 \rangle_M}{7!} Q^6 + \dots (11)$$

$$\frac{-1^n}{n!} \frac{d^n G_E}{d(Q^2)^n}(0) = \frac{\langle r^{2n} \rangle_E}{(2n+1)!}, (12)$$

$$\frac{-1^n}{n! \mu} \frac{d^n G_M}{d(Q^2)^n}(0) = \frac{\langle r^{2n} \rangle_M}{(2n+1)!}. (13)$$

For the details of the assumptions that go into these relations see Ref. [32].

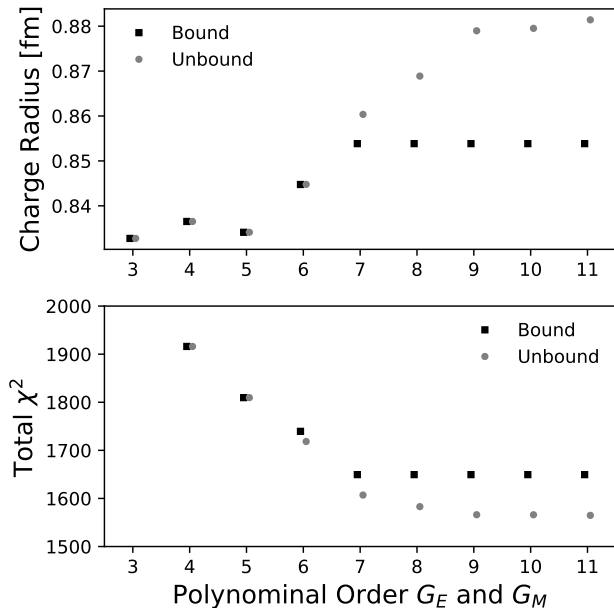


FIG. 4. Plotted is the total  $\chi^2$  for both the bounded and unbounded polynomial regressions of the full 1422 point Mainz data set. As shown, total  $\chi^2$  will continue to decrease as parameters are added though at some point no significant improvement will be made where significance is defined using a statistics test such as an F-Test, AIC and/or BIC [30]. Interestingly, the leading terms of both the bounded and unbounded fits follow the expected physical behavior until 7<sup>th</sup> order. With model selection using AIC or BIC, the bounded fits should be stopped at 7<sup>th</sup> order while the unbounded descriptive fits should be stopped at 10<sup>th</sup>.

In Table V we show how these terms shift for the bounded and unbounded fits of the original [20] and rebinned [13] Mainz data. It is also worth noting that negative values of the magnetic form factor are nonphysical. This should make it clear that polynomial regressions do not extract moments independently of the radius being extracted, and thus those trying to extract the radius in an impartial way from experimental data should not simply fix the higher order parameters based on a previous polynomial regression even though it has been done in numerous works [34–37]. In fact, based on the theory calculations of Alarcón and Weiss [33], it seems extremely unlikely that any high-order polynomial regressions of experimental data give access to the extremely complex true underlying moments. Thus, it seems far more likely that polynomial regressions, especially the unbounded ones, are simply descriptive fits of the experimental data and should be treated as such [38].

## IX. TEST DATA

Another tool of building predictive models, as opposed to a descriptive model, is to use data that was never used

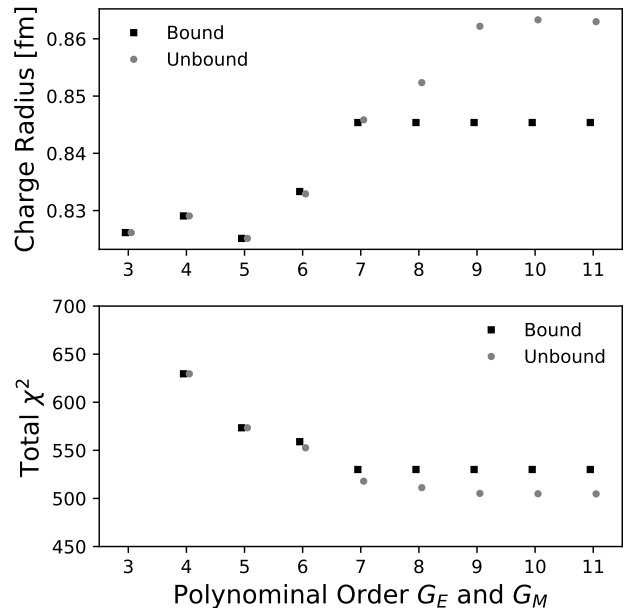


FIG. 5. Plotted is the total  $\chi^2$  for both the bounded and unbounded polynomial regressions of the 658 points of the rebinned Mainz data set [13]. It is disconcerting that with a reasonable rebinning of the data, the radius one would extract shifts for both the bounded and unbounded regressions. For these fits, by AIC and BIC, 7<sup>th</sup> order is the most appropriate for the bounded regression while for the unbounded 9<sup>th</sup> order is the most appropriate.

in the regressions to test how well the model generalizes. As shown in Fig. 7, we can use modern high precision low  $Q^2$  asymmetry measurements, measurements that are proportional to the ratio of the  $\mu G_E/G_M$ , to see how well our four regressions generalize.

At moderate  $Q^2$  all the curves do a reasonable job. However at higher  $Q^2$ , as one might expect from a high-order polynomial, none do particularly well. At low  $Q^2$ , where the magnetic form factor is not well constrained by either cross section or asymmetry data, it is interesting to note that the functions that are smooth in this region give small charge radii 0.854 fm for the original and 0.845 fm for the rebinned data; while the oscillatory unbounded fits give the systematically larger charge radii of 0.882 fm and 0.863 fm respectively. The magnetic radii give values of approximately 0.81 fm for the bounded fits and approximately 0.76 fm for the unbounded. This shows how high-precision low  $Q^2$  experimental asymmetry data will be extremely useful for selecting between these models.

## X. IMPORTANCE OF PHYSICAL MODELS

This example illustrates that it can be very challenging to understand the physical meaning of results when doing

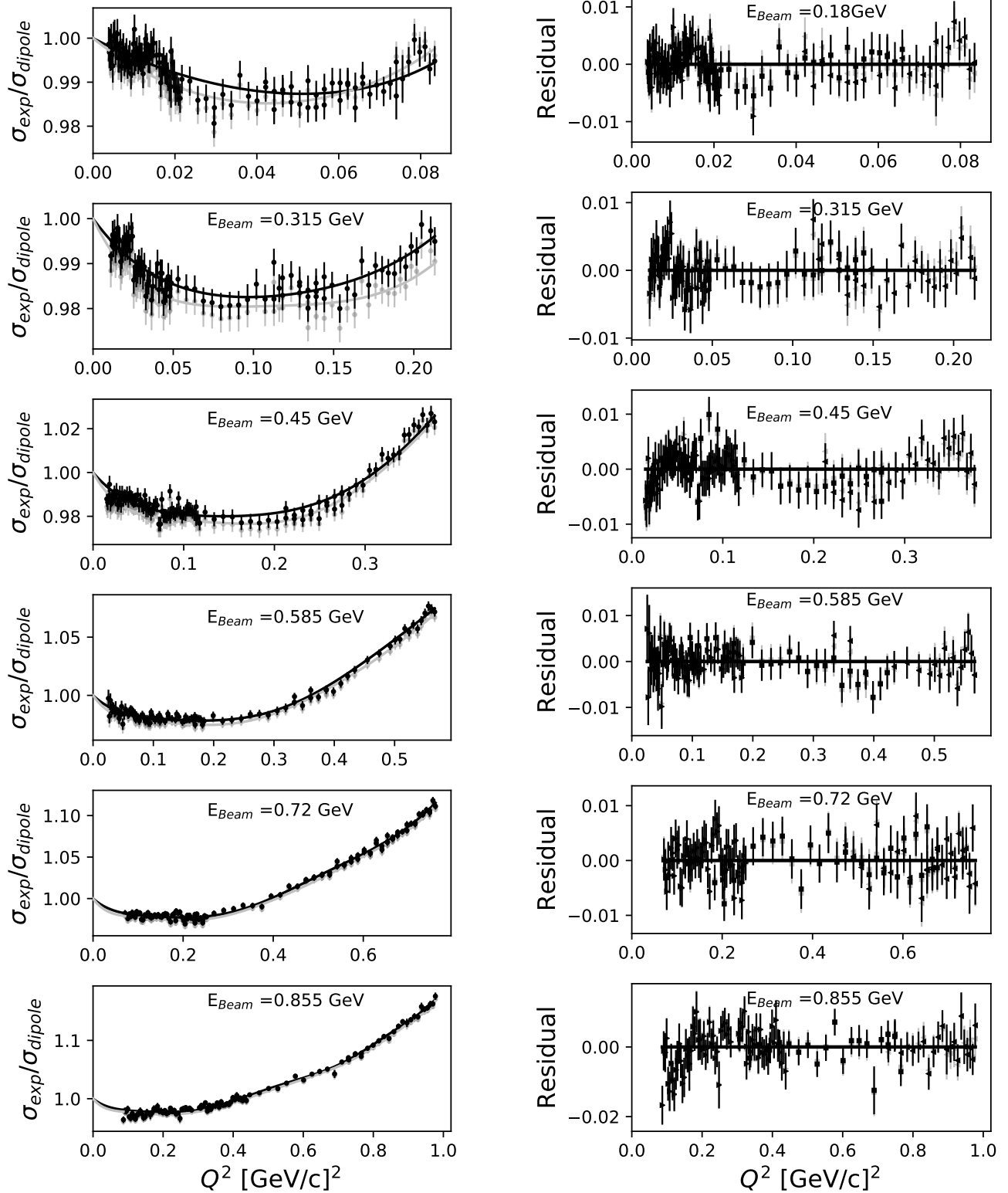


FIG. 6. Shown are the rebinned 658 cross section points analyzed with the two different analytic choices. The grey points were analyzed using an unconstrained eleventh order polynomial in  $G_E$  and  $G_M$  while the black points used a bounded regression: one constrained to be continuously monotone. The systematic difference in the location of the points is due to how the 31 normalization parameters are affected by the choice of regression function. While these means are again very different for the two fits, the residuals of the fits to their respective functions are amazingly similar.

TABLE IV. The values of the polynomial terms for the unconstrained and constrained regressions following the notation of Eq. 3 and 4 for the 658 points of rebinned data [13]. If one wishes to interpret the charge form factor slope term ( $i = 1$ ) in terms of charge radius using Eq. 1, one finds the unbound fit gives a charge radius of 0.863 fm while the bound, continuously monotone fit gives a radius of 0.845 fm.

i	unbound		bound	
	$a_i^E$	$a_i^M$	$a_i^E$	$a_i^M$
1	-3.19127	-2.46540	-3.06116	-2.76018
2	10.82576	-0.72681	8.41269	4.97927
3	-44.58633	35.31550	-24.45775	-5.19625
4	157.22016	-136.38607	58.22660	2.19337
5	-404.22137	228.82482	-89.35839	-0.00000
6	712.56978	-98.11370	74.77433	0.50348
7	-733.14790	-234.09993	-25.72800	-0.53301
8	133.43961	349.90224	0.00000	0.00000
9	632.78496	-122.36794	-0.00000	-0.00001
10	-695.45265	-56.48797	0.00001	0.00001
11	232.85612	35.79737	-0.00000	-0.00000

TABLE V. Moments from the four different  $11^{th}$  order polynomial fits are presented. Since all the moments change with the different fits, it is clearly inappropriate to fix the higher order terms to a particular value if one wishes to extract the radius, which is proportional to the  $\langle r^2 \rangle$  first term, in an unbiased manner. Now while these terms are the moments of the polynomial fit function (descriptive fitting), theory calculations such as those of Alarcón and Weiss [32, 33] would suggest that these terms, especially as the order increases, have little connection to the true underlying moments of the form factors.

moment	Original Cross Sections				Rebinned Cross Sections			
	unbound		bound		unbound		bound	
	$G_E$	$G_M$	$G_E$	$G_M$	$G_E$	$G_M$	$G_E$	$G_M$
$\langle r^2 \rangle \text{ fm}^2$	0.777	0.589	0.729	0.654	0.745	0.576	0.714	0.644
$\langle r^4 \rangle \text{ fm}^4$	2.33	-0.128	1.60	0.943	1.97	-0.132	1.52	0.905
$\langle r^6 \rangle \text{ fm}^6$	18.9	-11.9	7.64	1.70	13.2	-10.5	7.26	1.54
$\langle r^8 \rangle \text{ fm}^8$	207	-146	50.0	2.33	131	-113	48.4	1.82

non-linear regressions with many free parameters. This is particularly true of weighted least squares regressions where the fits are easily influenced by outlier points and reduced  $\chi^2$  cannot be used for determining the best non-linear model [26]. Different functions, limits, and bounds can easily lead to confirmation bias and a misinterpretation and/or inappropriate rejection of results. And as Johnny von Neumann is credited with saying, “With four parameters I can fit an elephant, and with five I can make him wiggle his trunk [43]” so it is perhaps not surprising that with such extremely complex regressions, nearly any plausible radius can be found.

Enrico Fermi noted that these types of problems should

be addressed using either a firm mathematical basis or a physical model. Thus, rather than debating which of

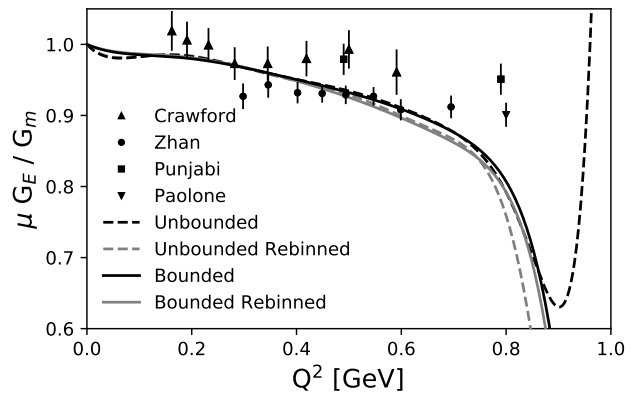


FIG. 7. Here we show high-precision elastic scattering asymmetry measurement results from Crawford [39], Zhan [40], Punjabi [41] and Paolone [42], data that has not been included in our fits, along with the four  $11^{th}$  order polynomial fits of the Mainz data.

the extremely complex non-linear regressions presented herein has the most merit, it is more appropriate to limit the analysis such that the analytical choices do not so strongly affect the results. To do this, we can either fit only lower  $Q^2$  data where fewer free parameters are required [11, 12, 23, 30, 44–49] and the results are not sensitive to the magnetic form factor, as shown explicitly in Ref. [30]; or, as Fermi preferred, use a physical model, such as that of Bernard *et al.* [50] or Alarcón and Weiss [33] to constrain the fits [16, 17, 51, 52]. There are also the physically motivated functions such as rational functions [12, 53] or continued fractions [11, 54, 55] though these still require model selection techniques to determine the appropriate number of regression parameters. Otherwise, by using extremely complex non-linear regressions and deep searches, one can choose to find nearly any radius from a single set of data [56]. To quote Nobel laureate Ronald H. Coase, “if you torture the data long enough, it will confess.”

## ACKNOWLEDGMENTS

Many thanks to Franziska Hagelstein and Vladimir Pascalutsa for their questions about normalization parameters that prompted this work. Thanks to Dave Meekins for his many useful comments and discussions. Thanks to Nigel Tufnel for suggesting going to eleven. And thanks to Marcy Stutzman and Simon Širca for their editorial comments. This work was supported by the U.S. Department of Energy contract DE-AC05-06OR23177 under which Jefferson Science Associates operates the Thomas Jefferson National Accelerator Facility.

- [1] R. Silberzahn *et al.*, *Advances in Methods and Practices in Psychological Science* **1**, 337 (2018), <https://doi.org/10.1177/2515245917747646>.
- [2] G. Shmueli, *Statist. Sci.* **25**, 289 (2010).
- [3] R. Pohl *et al.*, *Nature* **466**, 213 (2010).
- [4] A. Antognini *et al.*, *Science* **339**, 417 (2013).
- [5] P. J. Mohr, D. B. Newell, and B. N. Taylor, *Rev. Mod. Phys.* **88**, 035009 (2016), arXiv:1507.07956 [physics.atom-ph].
- [6] R. Pohl, R. Gilman, G. A. Miller, and K. Pachucki, *Ann. Rev. Nucl. Part. Sci.* **63**, 175 (2013), arXiv:1301.0905 [physics.atom-ph].
- [7] C. E. Carlson, *Prog. Part. Nucl. Phys.* **82**, 59 (2015), arXiv:1502.05314 [hep-ph].
- [8] G. A. Miller, in *13th Conference on the Intersections of Particle and Nuclear Physics (CIPANP 2018) Palm Springs, California, USA, May 29-June 3, 2018* (2018) arXiv:1809.09635 [physics.atom-ph].
- [9] G. A. Miller, *Phys. Rev.* **C99**, 035202 (2019), arXiv:1812.02714 [nucl-th].
- [10] M. Horbatsch and E. A. Hessels, *Phys. Rev.* **C93**, 015204 (2016), arXiv:1509.05644 [nucl-ex].
- [11] K. Griffioen, C. Carlson, and S. Maddox, *Phys. Rev.* **C93**, 065207 (2016), arXiv:1509.06676 [nucl-ex].
- [12] D. W. Higinbotham, A. A. Kabir, V. Lin, D. Meekins, B. Norum, and B. Sawatzky, *Phys. Rev.* **C93**, 055207 (2016), arXiv:1510.01293 [nucl-ex].
- [13] G. Lee, J. R. Arrington, and R. J. Hill, *Phys. Rev.* **D92**, 013013 (2015), arXiv:1505.01489 [hep-ph].
- [14] K. M. Graczyk and C. Juszczak, *Phys. Rev.* **C90**, 054334 (2014), arXiv:1408.0150 [hep-ph].
- [15] I. T. Lorenz and Ulf-G. Meißner, *Phys. Lett.* **B737**, 57 (2014), arXiv:1406.2962 [hep-ph].
- [16] M. Horbatsch, E. A. Hessels, and A. Pineda, *Phys. Rev.* **C95**, 035203 (2017), arXiv:1610.09760 [nucl-th].
- [17] J. M. Alarcn, D. W. Higinbotham, C. Weiss, and Z. Ye, *Phys. Rev.* **C99**, 044303 (2019), arXiv:1809.06373 [hep-ph].
- [18] S. Zhou, P. Giuliani, J. Piekarewicz, A. Bhattacharya, and D. Pati, *Phys. Rev. C* (2019), arXiv:1808.05977 [nucl-th].
- [19] J. C. Bernauer *et al.* (A1), *Phys. Rev. Lett.* **105**, 242001 (2010), arXiv:1007.5076 [nucl-ex].
- [20] J. C. Bernauer *et al.* (A1), *Phys. Rev.* **C90**, 015206 (2014), arXiv:1307.6227 [nucl-ex].
- [21] M. Merkle, in *Analytic Number Theory, Approximation Theory, and Special Functions*, edited by G. V. Milovanović and M. T. Rassias (Springer-Verlag New York, New Your, 2012) Chap. 12, pp. 347–364, arXiv:1211.0900.
- [22] W. H. Press, S. A. Teukolsky, W. T. Vetterling, and B. P. Flannery, *Numerical Recipes 3rd Edition: The Art of Scientific Computing*, 3rd ed. (Cambridge University Press, New York, NY, USA, 2007).
- [23] X. Yan, D. W. Higinbotham, D. Dutta, H. Gao, A. Gasparian, M. A. Khandaker, N. Liyanage, E. Pasyuk, C. Peng, and W. Xiong, *Phys. Rev.* **C98**, 025204 (2018), arXiv:1803.01629 [nucl-ex].
- [24] J. J. Koehler, *Organizational Behavior and Human Decision Processes* **56**, 28 (1993).
- [25] J. P. A. Ioannidis, *PLOS Medicine* **2** (2005), 10.1371/journal.pmed.0020124.
- [26] R. Andrae, T. Schulze-Hartung, and P. Melchior, *ArXiv e-prints* (2010), arXiv:1012.3754 [astro-ph.IM].
- [27] F. J. Anscombe, *The American Statistician* **27**, 17 (1973).
- [28] H. Akaike, *IEEE Transactions on Automatic Control* **19**, 716 (1974).
- [29] G. Schwarz, *Ann. Statist.* **6**, 461 (1978).
- [30] D. W. Higinbotham, P. Giuliani, R. E. McClellan, S. Sirca, and X. Yan, (2018), arXiv:1812.05706 [physics.data-an].
- [31] R. Andrae, T. Schulze-Hartung, and P. Melchior, *ArXiv e-prints*, arXiv:1012.3754 (2010), arXiv:1012.3754 [astro-ph.IM].
- [32] J. M. Alarcón and C. Weiss, *Phys. Rev.* **C97**, 055203 (2018), arXiv:1710.06430 [hep-ph].
- [33] J. M. Alarcón and C. Weiss, *Phys. Lett.* **B784**, 373 (2018), arXiv:1803.09748 [hep-ph].
- [34] R. Rosenfelder, *Phys. Lett.* **B479**, 381 (2000), arXiv:nucl-th/9912031 [nucl-th].
- [35] M. Mihovilović *et al.*, *Phys. Lett.* **B771**, 194 (2017), arXiv:1612.06707 [nucl-ex].
- [36] I. Sick and D. Trautmann, *Phys. Rev.* **C95**, 012501 (2017), arXiv:1701.01809 [nucl-ex].
- [37] S. Belostotski, N. Sagidova, and A. Vorobyev, (2019), arXiv:1903.04975 [hep-ph].
- [38] Perhaps even more surprisingly, even if we had the true moments, they do not necessarily uniquely determine the generating function (see page 378 of Ref. [57]). In other words, while functions can have moments; moments do not uniquely determine functions.
- [39] C. B. Crawford *et al.*, *Phys. Rev. Lett.* **98**, 052301 (2007), arXiv:nucl-ex/0609007 [nucl-ex].
- [40] X. Zhan *et al.*, *Phys. Lett.* **B705**, 59 (2011), arXiv:1102.0318 [nucl-ex].
- [41] V. Punjabi *et al.*, *Phys. Rev.* **C71**, 055202 (2005), [Erratum: *Phys. Rev. C*71,069902(2005)], arXiv:nucl-ex/0501018 [nucl-ex].
- [42] M. Paolone *et al.*, *Phys. Rev. Lett.* **105**, 072001 (2010), arXiv:1002.2188 [nucl-ex].
- [43] F. Dyson, *Nature* **427**, 297 EP (2004).
- [44] L. N. Hand, D. G. Miller, and R. Wilson, *Rev. Mod. Phys.* **35**, 335 (1963).
- [45] J. J. Murphy, Y. M. Shin, and D. M. Skopik, *Phys. Rev.* **C9**, 2125 (1974), [Erratum: *Phys. Rev. C*10, 2111 (1974)].
- [46] F. Borkowski, G. G. Simon, V. H. Walther, and R. D. Wendling, *Z. Phys.* **A275**, 29 (1975).
- [47] G. G. Simon, C. Schmitt, F. Borkowski, and V. H. Walther, *Nucl. Phys.* **A333**, 381 (1980).
- [48] F. Hagelstein and V. Pascalutsa, (2018), arXiv:1812.02028 [nucl-th].
- [49] T. B. Hayward and K. A. Griffioen, (2018), arXiv:1804.09150 [nucl-ex].
- [50] V. Bernard, H. W. Fearing, T. R. Hemmert, and Ulf-G. Meißner, *Nucl. Phys.* **A635**, 121 (1998), [Erratum: *Nucl. Phys. A*642,563(1998)], arXiv:hep-ph/9801297 [hep-ph].
- [51] G. Hohler, E. Pietarinen, I. Sabba Stefanescu, F. Borkowski, G. G. Simon, V. H. Walther, and R. D. Wendling, *Nucl. Phys.* **B114**, 505 (1976).

- [52] I. T. Lorenz, Ulf.-G. Meißner, H. W. Hammer, and Y. B. Dong, Phys. Rev. **D91**, 014023 (2015), arXiv:1411.1704 [hep-ph].
- [53] J. J. Kelly, Phys. Rev. **C70**, 068202 (2004).
- [54] I. Sick, Phys. Lett. **B576**, 62 (2003), arXiv:nucl-ex/0310008 [nucl-ex].
- [55] I. T. Lorenz, H. W. Hammer, and Ulf.-G. Meißner, Eur. Phys. J. **A48**, 151 (2012), arXiv:1205.6628 [hep-ph].
- [56] D. W. Higinbotham, (2019), 10.5281/zenodo.2566639.
- [57] S. Širca, *Probability for Physicists*, Graduate Texts in Physics (Springer International Publishing, 2016).